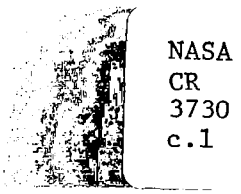

NASA Contractor Report 3730

A Method for Computing the Leading-Edge Suction in a Higher-Order Panel Method

F. Edward Ehlers and Marjorie E. Manro

CONTRACT NAS1-16740
MARCH 1984

NASA

NASA Contractor Report 3730

A Method for Computing the Leading-Edge Suction in a Higher-Order Panel Method

F. Edward Ehlers and Marjorie E. Manro
Boeing Commercial Airplane Company
Seattle, Washington

Prepared for
Langley Research Center
under Contract NAS1-16740

National Aeronautics
and Space Administration

**Scientific and Technical
Information Office**

1984

CONTENTS

TABLES

FIGURES

SUMMARY

Experimental data show that the phenomenon of a separation-induced leading-edge vortex is influenced by the wing thickness and the shape of the leading edge. Both thickness and leading-edge shape (rounded rather than pointed) delay the formation of a vortex.

The theoretical methods for calculating the effects of a leading-edge vortex do not include a procedure for determining if a vortex exists. Under a previous NASA contract (ref. 1), it was established that the start of the vortex can be predicted by using the relationship between the leading-edge suction coefficient and the parabolic nose drag. In that contract, the leading-edge suction was calculated by using the results of a linear theory.

This study has been made to develop a method for calculating the leading-edge suction in the same computer code that calculates the pressure distribution due to the leading-edge vortex. As the exact calculation is complex, involving a fourfold integration, the approach was to find a numerical procedure that takes advantage of the capability of the Leading-Edge Vortex (LEV) Program to evaluate flow-field properties at arbitrary points.

The numerical procedures were developed for a two-dimensional case; all evaluations used a two-dimensional flat plate as the model. As a result, it was determined that a Gaussian quadrature is the preferred method, as it was derived specifically with a logarithmic singularity at each panel edge. The method has not been evaluated in a three-dimensional environment.

INTRODUCTION

The theoretical methods used to predict the effect of a leading-edge vortex do not determine that a vortex is present. Experimental data show that the formation and development of a leading-edge vortex is delayed on a wing with thickness. On these configurations the vortex starts to form near the wingtip at moderate angles of attack and moves inboard as the angle of attack increases. There is, therefore, a need for a method to determine the portion of the semispan over which the vortex exists at each angle of attack.

The position of the vortex is influenced by the aeroelastic distortion as well as by wing thickness. Work performed under a previous NASA contract (NAS1-15678, ref. 1) used the pressure distributions predicted by the linear theory FLEXSTAB (ref. 2), in conjunction with the parabolic nose drag, to predict the location of the vortex. This method was quite successful but it is inconsistent to use FLEXSTAB with a separated-flow method.

The current study was made to develop a method for calculating the leading-edge suction using the same computer code that is used for the separated-flow case (the Leading-Edge Vortex (LEV) Program, refs. 3 and 4). The initial plan was to use the method currently available in PAN AIR (ref. 5). Analysis of this method for calculating leading-edge suction, showed that the linear extrapolation of doublet strength/ $\sqrt{x}$ for the two panels closest to the edge is incorrect, partially because the doublet strength is actually represented by a quadratic polynomial. In the PAN AIR code, this calculated suction is modified by a factor that varies with the panel density and the type of panel spacing (i.e., uniform, cosine, or semicosine). This modification is intended to correct the erroneous assumption of linear variation of doublet strength/ $\sqrt{x}$ but it does not provide corrections for arbitrary paneling arrangements.

Consideration was then given to an exact calculation of the leading-edge suction. This is a complex task because it requires the integration, over a surface, of functions that are also surface integrals, i.e., a fourfold integration. For panels far from the leading edge, the integrals may be evaluated numerically. This is the current approach to the evaluation of forces in the LEV code. Near the leading edge, care must be taken due to the logarithmic singularity in the $\vec{V}$ and $\vec{W} \cdot \hat{n}$ terms. The correct result will be obtained if evaluated analytically.

The formulation of the exact calculation of leading-edge suction for the three- dimensional case would require a large amount of time, therefore, an investigation of other approaches seemed advisable. The capability is available in the LEV Program to evaluate the flowfield properties that are required for the leading-edge suction calculation, at points other than the control points on the networks defined for the solution (off-body points). The formulation of the problem is much simpler for a two-dimensional case than for a three-dimensional case. What may be considered a two-dimensional version of the LEV Program, including the off-body capability, is available as a computer code. For these reasons, the following development assumes two-dimensional flow. The development of procedures for using these additional points to calculate the leading-edge suction is described in the next section. The study included an evaluation of the number of points, distribution of points on the panels, and integration method required to calculate an adequate leading-edge suction coefficient.

SYMBOLS

b	wing span
c	chord
$C_{D,p}$	pressure drag coefficient
C_L	lift coefficient
C_S	leading-edge suction coefficient
$\vec{F}$	force vector
F_L	lift
F_S	suction force
M_∞	free stream Mach number
$\hat{n}$	surface unit normal vector
p	pressure
S	singularity surface
$\vec{v}$	perturbation velocity
$\vec{V}$	total velocity
$\vec{V}_\infty$	free stream velocity
$\vec{w}$	perturbation mass flux vector
$\vec{W}$	total mass flux vector
wt	weighting factor in Gaussian quadrature
x,y,z	Cartesian coordinates
α	angle of attack
β	$\sqrt{1 - M_\infty^2}$

SYMBOLS (Concluded)

μ	doublet strength
ρ_∞	free stream fluid density
ϕ	perturbation potential
(ϕ_x,ϕ_y,ϕ_z)	gradient of perturbation potential

FORMULATION OF THE GENERAL SOLUTION

Euler's momentum theorem states that the force on a body can be determined by integrating the pressure and momentum through any surface S enclosing the body:

$$\vec{F} = -\int_S \left[p\,\hat{n} + (\rho\,\vec{V}\cdot\hat{n})\,\vec{V} \right] ds \tag{1}$$

When the pressure p is given by the quadratic relation, the formula holds for linearized theory as well and the formula takes the form

$$\vec{F} = -\int_S \left[p\,\hat{n} + (\vec{W}\cdot\hat{n})\,\vec{V} \right] ds \tag{2}$$

where:

$$\vec{W} = \vec{W}_\infty + \vec{w}$$

$$\vec{V} = \vec{V}_\infty + \vec{v}$$

$$\vec{W}_\infty = \rho_\infty \vec{V}_\infty$$

$$\vec{V} = (\phi_x, \phi_y, \phi_z)$$

$$\vec{W} = (\beta^2\phi_x, \phi_y, \phi_z)$$

$$\beta^2 = 1 - M_\infty^2$$

$$p = p_\infty + \frac{1}{2}\rho_\infty \left[-2\,V_\infty \phi_x + \beta^2\phi_x^2 + \phi_y^2 + \phi_z^2 \right]$$

The boundary condition of impermeability on the body is given by

$$\vec{W}\cdot\hat{n} = 0.0 \tag{3}$$

The surface S may be moved to the wing surface if the product of $\vec{v}$ and $\vec{w}$ is integrable. For the flat plate the integration of the pressure over the wing produces only a component normal to the plate. There is a branch point singularity at the leading edge and the integral around a small circle whose radius is reduced to zero about the leading edge yields a component of the force parallel to the plate. For the panel method, $\vec{w}$ has a logarithmic singularity and the integration around the leading edge vanishes as the radius of the circle is reduced to zero. However, there is a contribution to the tangential force from the tip region because the normal mass flux vector $\vec{W}\cdot\hat{n}$ is not zero. The normal mass flux vector is zero only at the control points on the wing. On the edge panel, however, the mass flux vector goes to infinity logarithmically as the leading edge is approached. Hence there is a contribution from the momentum integral from the section of the leading edge between the leading edge and the first inboard control point. Let S be the two sides of the flat plate wing and wake, then equation (2) becomes

$$\vec{F} = -\int_0^{b/2}\int_0^{\infty} \left[p^+ \hat{n} + (\vec{W}^+ \cdot \hat{n})\,\vec{V}^+ - p^- \hat{n} - (\vec{W}^- \cdot \hat{n})\,\vec{V}^-\right] ds \tag{4}$$

where the plus sign denotes upper surface values and the minus sign denotes the lower surface values. But as $\vec{W}^+ \cdot \hat{n} = \vec{W}^- \cdot \hat{n}$ is a property of the doublet sheet, this can be simplified to

$$\vec{F} = -\int_0^{b/2}\int_0^{\infty} \left[\Delta p\, \hat{n} + (\vec{W} \cdot \hat{n})\,\Delta\vec{V}\right] ds \tag{5}$$

where $\Delta p = p^+ - p^-$ and $\Delta\vec{V} = \vec{V}^+ - \vec{V}^-$.

Assuming that the contribution to $\vec{W}\cdot\hat{n}$ from surrounding panels varies slowly over the panel between the control point and the leading edge, and since the contribution over the panel itself dominates,

$$\vec{W} \cdot \hat{n} = \vec{W}_{cp} \cdot \hat{n} + (\vec{W} \cdot \hat{n} - \vec{W}_{cp} \cdot \hat{n}) \tag{6}$$

where the subscript cp denotes the value at the control point. The first term on the right hand side vanishes because of the applied boundary condition $\vec{W}\cdot\hat{n} = 0$. Hence for the flat plate at $M_\infty = 0.0$,

$$\vec{W} \cdot \hat{n} = \rho_\infty \left[\phi_z - (\phi_z)_{cp}\right] \tag{7}$$

In panel components, $\Delta\vec{V} = (\mu_x, \mu_y, 0)$, where μ is the value of the doublet strength on the plate. Since ds = dx dy, the contribution to the force from the wing at the leading edge is

$$\vec{F}_S = -\rho_\infty \int_0^{b/2}\int_0^{x_{cp}} (\mu_x, \mu_y, 0)\left[\phi_z - (\phi_z)_{cp}\right] dx\, dy \tag{8}$$

where the integration is over the region near the leading edge between the line of control points on the edge panels and the leading edge.

CALCULATION OF LEADING-EDGE SUCTION ON A TWO-DIMENSIONAL FLAT PLATE

EXACT SOLUTION

The two-dimensional incompressible flow over a flat plate at an angle of attack can be obtained from the flow around a circle with circulation by a simple conformal mapping. The complex function which maps a circle in the S plane into a flat plate in the z plane is given by

$$z = \zeta + a^2 / \zeta \tag{9}$$

$$\frac{dz}{d\zeta} = (\zeta^2 - a^2) / \zeta^2 \tag{10}$$

The complex potential $f(\zeta)$ for the flow around a circle of radius a at an angle of attack α with circulation Γ is

$$f(\zeta) = \zeta\, e^{-i\alpha} + a^2 e^{i\alpha}/\zeta + (i\,\Gamma / 2\,\pi) \log (\zeta / a) \tag{11}$$

The velocity in the physical z plane is found by differentiation of equation (11) with respect to z or

$$\frac{df}{dz} = \frac{df}{d\zeta}\frac{d\zeta}{dz} = \left[e^{-i\alpha} - a^2 e^{i\alpha} / \zeta^2 + i\,\Gamma / 2\,\pi\,\zeta\right] \zeta^2 / (\zeta^2 - a^2) \tag{12}$$

At the trailing edge, df/dz must be finite, therefore

$$e^{-i\alpha} - e^{i\alpha} + i\,\Gamma / 2\,\pi\, a = 0.0 \tag{13}$$

or

$$\Gamma = 4\,\pi\, a \sin\alpha \tag{14}$$

Then, by substitution of equation (14) into equation (11), the complete complex potential becomes

$$f(\zeta) = \zeta\, e^{-i\alpha} + a^2 e^{i\alpha} / \zeta + 2\, i\, a \sin\alpha \log (\zeta / a) \tag{15}$$

The complex force vector $\overline{F}$ is found from the Blasius formula:

$$\overline{F} = \left(\frac{1}{2} i\, \rho_\infty\, V_\infty^2\right) \oint \left(\frac{df}{dz}\right)^2 dz = \left(\frac{1}{2} i\, \rho_\infty\, V_\infty^2\right) \oint \left(\frac{df}{d\zeta}\right)^2 \left(\frac{d\zeta}{dz}\right) d\zeta \tag{16}$$

The integrand on the right is seen to be

$$\left[e^{-i\alpha} - a^2 e^{i\alpha} / \zeta^2 + 2\,i\,a \sin\alpha / \zeta\right]^2 \zeta^2 / (\zeta^2 - a^2) \tag{17}$$

Near the origin this becomes

$$-\left[e^{-2i\alpha}\zeta^2 + a^4 e^{2i\alpha} / \zeta^2 - 4\,a^2 \sin^2\alpha - 2\,a^2 + 4\,i\,a\,e^{-i\alpha}\,\zeta \sin\alpha \right.$$
$$\left. - 4\,i\,a^3 e^{i\alpha} \sin\alpha / \zeta\right] / a^2 + 0(1) \tag{18}$$

This expression has a pole at the origin of the circle plane whose residue is given by

$$4\,i\,a\,e^{i\alpha} \sin\alpha \tag{19}$$

Integration around the pole at $\zeta = 0$ yields

$$-8\,\pi\,a\,e^{i\alpha} \sin\alpha \tag{20}$$

The integrand also has a pole at $\zeta = -a$ but not at $\zeta = a$. By factoring the quantity in square brackets (eq. 18), the following is obtained

$$\left[(e^{-i\alpha} / \zeta^2)(\zeta - a)(\zeta + a\,e^{2i\alpha})\right]^2 \zeta^2 / (\zeta^2 - a^2) \tag{21}$$

The residue at $\zeta = -a$ is seen to be

$$8\,a \sin^2\alpha \tag{22}$$

Integration of equation (16) finally yields

$$\overline{F} = \left(\frac{1}{2}\rho_\infty V_\infty^2\right) 8\,\pi\,a\left[-\sin^2\alpha - i \sin\alpha \cos\alpha\right] \tag{23}$$

which simplifies to

$$F = \left(\frac{1}{2}\rho_\infty V_\infty^2\right) 8\,\pi\,a\,i\,e^{i\alpha} \sin\alpha \tag{24}$$

The suction term is the real part: $F_S = -\left(\frac{1}{2}\rho_\infty V_\infty^2\right) 8\,\pi\,a \sin^2\alpha$

and the lift is the imaginary part: $F_L = \left(\frac{1}{2}\rho_\infty V_\infty^2\right) 8\,\pi\,a \cos\alpha \sin\alpha$

Since from the mapping, the chord of the wing is equal to 4a, the coefficients for the exact two-dimensional solution are as follows:

$$C_L = \pi \sin(2\alpha) \tag{25}$$

$$C_S = -2\pi \sin^2 \alpha \tag{26}$$

APPROXIMATE CLOSED FORM FORMULA

The perturbation potential produced by the doublet distribution from the leading-edge panel is given by

$$\phi = -\frac{1}{2\pi} \int_0^{x_{cp}} \mu(x_0) \frac{\partial}{\partial z_0} (\log r)\, dx_0 \tag{27}$$

where μ is the doublet strength and

$$r = \sqrt{(x - x_0)^2 + (z - z_0)^2} \tag{28}$$

Performing the differentiation yields

$$\phi = \frac{1}{2\pi} \int_0^{x_{cp}} \frac{\mu(x_0)(z \quad z_0)\, dx_0}{(x - x_0)^2 + (z - z_0)^2} \tag{29}$$

Let $(x - x_0)/(z - z_0) = t$ or $x_0 = x - t(z - z_0)$. On the plate, $z_0 = 0$, and

$$\phi = \frac{1}{2\pi} \int_{(x-x_{cp})/z}^{x/z} \mu(x - t\,z)\, dt / (t^2 + 1) \tag{30}$$

This equation may be tested by letting z go to zero through positive values yielding

$$\phi = \frac{\mu(x)}{2\pi} \int_{-\infty}^{\infty} \frac{dt}{(t^2 + 1)} = \frac{\mu(x)}{2} \tag{31}$$

Similarly, letting z go to zero through negative values,

$$\phi = \frac{\mu(x)}{2\pi} \int_{\infty}^{-\infty} \frac{dt}{(t^2 + 1)} = -\frac{\mu(x)}{2} \tag{32}$$

Thus the jump in potential across the plate is equal to the value of the doublet strength, as required.

To find the normal component of the velocity, equation (30) is differentiated with respect to z.

$$\phi_z = \frac{1}{2\pi}\left[\frac{\mu(o)}{(x/z)^2+1}\left(-\frac{x}{z^2}\right) - \frac{\mu(x_{cp})}{\left(\frac{x-x_{cp}}{z}\right)^2+1}\left(-\frac{x-x_{cp}}{z^2}\right)\right.$$

$$\left. - \int_{(x-x_{cp})/z}^{x/z} \mu'(x - t\,z)\,t\,dt/(t^2+1)\right] \tag{33}$$

Since $\mu = 0$ at $x = 0$, then

$$\mu(x) = b\,x + c\,x^2 \tag{34}$$

for some coefficients b and c, and

$$\mu'(x) = b + 2\,c\,x \tag{35}$$

Thus

$$\mu'(x - t\,z)\,t = (b + 2\,c\,x)\,t - 2\,c\,z\,t^2 \tag{36}$$

The integral in equation (33) becomes

$$\int_{(x-x_{cp})/z}^{x/z} \mu'(x - t\,z)\,t\,dt/(t^2+1) = \frac{b + 2\,c\,x}{2}\log\left[\frac{x^2+z^2}{(x-x_{cp})^2+z^2}\right]$$

$$- 2\,c\,z\left[\frac{x}{z} - \frac{(x-x_{cp})}{z} + \tan^{-1}\left(\frac{x}{z}\right) - \tan^{-1}\left(\frac{x-x_{cp}}{z}\right)\right] \tag{37}$$

Substituting equation (37) into equation (33) yields

$$\phi_z = \frac{1}{2\pi}\left\{\frac{\mu(x_{cp})(x-x_{cp})}{(x-x_{cp})^2+z^2} - \frac{\mu'(x)}{2}\log\left[\frac{x^2+z^2}{(x-x_{cp})^2+z^2}\right]\right.$$

$$\left. + 2\,c\,z\left[\frac{x_{cp}}{z} + \tan^{-1}\left(\frac{x}{z}\right) - \tan^{-1}\left(\frac{x-x_{cp}}{z}\right)\right]\right\} \tag{38}$$

Let z go to zero. This leads to

$$\phi_z = -\frac{1}{2\pi}\mu'(x)\log x + (\text{terms in } x_{cp}) \tag{39}$$

The terms involving x_{cp} are cancelled by the contribution from the adjoining panel.

The leading edge suction is then approximately given by substituting equation (39) into equation (8), namely,

$$F_S = \left(\frac{\rho_\infty}{2\pi}\right)\int_0^{x_{cp}} \mu'(x)\left[\mu'(x)\log x - \mu'(x_{cp})\log x_{cp}\right]dx \tag{40}$$

Integration and simplification lead to the following formula for the suction force coefficient:

$$C_S = -\frac{1}{\pi V_\infty^2}\left[c\,x_{cp}^2\left(b + \frac{2\,c\,x_{cp}}{3}\right)\log x_{cp} + b\,x_{cp}\,(b + c\,x_{cp}) + \frac{4\,c^2\,x_{cp}^3}{9}\right] \tag{41}$$

where the coefficients b and c are obtained from equation (34) using values at the first control point and the trailing edge of the first panel.

NUMERICAL CALCULATION OF LEADING-EDGE SUCTION

The suction force coefficient C_s for the two-dimensional flat plate is determined by using the momentum integral

$$C_S = -\frac{2}{V_\infty^2}\int_0^{x_N} \mu'(x)\,W(x)\,dx \tag{42}$$

where μ is the doublet strength, W the normal total mass flux, and x_N is the first control point inboard of the leading edge and for which $W(x_N)$ is zero. The values of $\mu(x_i)$ and $W(x_i)$ are evaluated at specified values of x_i and z_i. As mentioned before, the capability to solve for these quantities at locations other than control points is available in the LEV Program as well as in the two-dimensional code used in this study. For the three-dimensional case, it is necessary to include y_i in defining the location at which flow field properties are desired. To avoid the singularities on the surface, the value of z_i must be chosen to be slightly above the surface (e.g., 0.000001). The integral from x_1 to x_N is calculated by numerical quadrature.

A logarithmic singularity occurs at the leading edge and the integral from the leading edge to x_1 is calculated analytically by using equation (41). Between 0 and x_1 we see from equations (39) and (35) that W varies like

$$(b + 2\,c\,x)\log x \tag{43}$$

Let $W(x)$ for $0 \leq x \leq x_1$ be given by

$$W(x) = W_1 - \frac{1}{2\pi}\mu'(x)\log x + \frac{1}{2\pi}\mu'(x_1)\log x_1 \tag{44}$$

It is clear that $W(x_1) = W_1$ as it should. The first step in the integration is

$$C_1 = -\frac{2}{V_\infty{}^2}\int_0^{x_1} \mu'(x)\,W(x)\,dx$$

$$= -\frac{1}{\pi V_\infty{}^2}\left[c\,x_1{}^2\left(b + \frac{2\,c\,x_1}{3}\right)\log x_1 + b\,x_1\,(b + c\,x_1) + \frac{4\,c^2\,x_1{}^3}{9}\right]$$

$$- \frac{2\,W_1\,\mu(x_1)}{V_\infty{}^2} \tag{45}$$

Then the suction coefficient is given by

$$C_S = C_1 - \frac{2}{V_\infty{}^2}\int_{x_1}^{x_N} \mu'(x)\,W(x)\,dx \tag{46}$$

where the integral can be computed numerically. The normal mass flux $W(x)$ and the doublet strength μ are evaluated at selected points by using the off-body capability in the computer code. Three standard methods were used in the evaluation. These are the trapezoidal rule, Simpson's rule, and a Gaussian quadrature formula.

TRAPEZOIDAL RULE

Using the trapezoidal rule, the integral of equation (46) is replaced by a summation and the term C_1 is calculated using equation (45). The formula for the trapezoidal rule is

$$C_S = C_1 - \frac{1}{V_\infty{}^2}\sum_{i=1}^{N-1}\left[\mu'(x_i)\,W(x_i) + \mu'(x_{i+1})\,W(x_{i+1})\right]\left(x_{i+1} - x_i\right) \tag{47}$$

SIMPSON'S RULE

With Simpson's rule, it is required that the length over which integration is to be done be divided into an even number of equal segments, i.e., $\Delta x = x_i - x_{i-1}$ for all values of i. The integral of equation (46) is again replaced by a summation and equation (45) is used for the term C_1 with the formula using Simpson's rule as follows:

$$C_S = C_1 - \frac{2}{V_\infty{}^2}\frac{\Delta x}{3}\left[\mu'(x_1)\,W(x_1) + \mu'(x_n)\,W(x_n)\right.$$

$$+ 4\left(\mu'(x_2)\,W(x_2) + \mu'(x_4)\,W(x_4) + \cdots + \mu'(x_{n-1})\,W(x_{n-1})\right)$$

$$\left. + 2\left(\mu'(x_3)\,W(x_3) + \mu'(x_5)\,W(x_5) + \cdots \mu'(x_{n-2})\,W(x_{n-2})\right)\right] \tag{48}$$

GAUSSIAN QUADRATURE

A Gaussian quadrature formula with weight functions determined by the logarithmic singularity may also be used. For this case the first step C_1 need not be computed. Consider the following integral:

$$\int_0^b \log x\, f(x)\, dx = \sum_{k=1}^{N} wt(k)\, f(x_k) \tag{49}$$

The weights wt and the abscissas x_k are chosen so that the relation above is exact for f(x) a polynomial of degree less than $2N - 1$. To compute these weights, the method of Desmarais (ref. 6) is used. A set of polynomials $p_n(x)$, orthogonal with respect to log x, is constructed, i.e.,

$$\int_0^b \log x\, p_n(x)\, p_m(x)\, dx = \delta_{nm}\, h_n \tag{50}$$

where $\delta_{nm} = 1$ if $m = n$, and $\delta_{nm} = 0$ if $m \neq n$.

These polynomials take the form

$$\left.\begin{aligned} p_0(x) &= 1.0 \\ p_1(x) &= x - b_1 \\ p_n(x) &= (x - b_n)\, p_{n-1}(x) - c_n p_{n-2}(x) \end{aligned}\right\} \tag{51}$$

where

$$\left.\begin{aligned} b_n &= h'_{n-1} / h_{n-1} \\ c_n &= h_{n-1} / h_{n-2} \end{aligned}\right\} \tag{52}$$

$$\left.\begin{aligned} h_n &= \int_0^b \log x\, p_n{}^2(x)\, dx \\ h_n{}' &= \int_0^b \log x\, p_n{}^2(x)\, x\, dx \end{aligned}\right\} \tag{53}$$

The abscissas are found by solving $p_n(x) = 0$. When these are obtained the weights are found by calculating

$$wt(k) = h_{n-1} / p_n{}'(x_k)\, p_{n-1}(x_k) \tag{54}$$

The integration of F(x) which has the logarithmic singularity at $x = 0$ is then found by

$$\int_0^b F(x)\, dx = \sum_{k=1}^{N} wt(k)\, F(x_k) / \log x_k \tag{55}$$

The variation of the mass flux W between the panel edge and the control point is the same as the variation of -log x between 0.0 and 1.0. Therefore, the limit b is chosen to be 1.0, and each half-panel is nondimensionalized on the length of that half-panel with the origin placed at the panel edge. This derivation for a single half-panel may be used over any half-panel if the origin is placed at the panel edge.

The locations along the chord at which the normal mass flux and doublet strength are required are determined, along with the weighting factors for each point, and the leading-edge suction coefficient is calculated as follows:

$$C_S = -\frac{2}{V_\infty{}^2}\,\frac{1}{c}\sum_{m=1}^{P} c_m \sum_{k=1}^{N} wt_k \frac{\mu'(x_{km})\, W(x_{km})}{\log (x_k)} \tag{56}$$

where:

c = total chord length

c_m = half-panel length

P = number of half-panels, always odd

N = number of points per half-panel used in Gaussian quadrature

x_k = fraction of the half-panel length with the origin at the panel edge

x_{km} = position based on total chord length, calculated as follows:

$$x_{km} = x_k\, c_m + \sum_{j=1}^{m-1} c_j \text{ , for half-panels forward of panel centroid (m odd)}$$

$$x_{km} = -\,x_k\, c_m + \sum_{j=1}^{m} c_j \text{ , for half-panels aft of panel centroid (m even)}$$

EVALUATION OF METHODS

The various procedures described have been used to evaluate the calculation of the leading-edge suction coefficient and yield results which are the same relative to the exact value of suction coefficient, regardless of the angle of attack. Therefore, the relative error of the calculated values is shown in tables 1 and 2. A two-dimensional flat plate at angle of attack was used as the test case for the evaluation of numerical solutions; all conditions were at M = 0.

Three numerical methods for calculating the leading-edge suction force were tried and compared to the exact theoretical values. These methods were the trapezoidal rule, Simpson's rule, and Gaussian quadrature; all require the values of doublet strength and downwash at specific points other than at the control points. Values of downwash and doublet strength were computed at these points using a current capability of the two-dimensional code that allows for the evaluation of flow field properties, i.e., mass flux components and pressure coefficients, at user-specified points in space (off-body points) in addition to the control points that are located at the panel midpoints.

In addition, a closed form approximation of the momentum integral was derived by integrating the product of the doublet gradient and the downwash over the region between the leading edge and the first (closest to the leading edge) control point or the most forward off-body point. Use of this formula, with no additional data for off-body points, grossly overpredicts the suction force as seen in table 1. It yields essentially the same results as obtained with the method currently used in PANAIR prior to the application of the correction factor. As off-body points cannot be evaluated exactly at the leading edge, this formula was used in the immediate vicinity of the leading edge as one term in the numerical solution of the momentum integral by the trapezoidal and Simpson's rules.

The chordwise distribution of panels used to define a configuration is completely at the option of the analyst. For the best prediction of the load distribution, the panels are generally smaller where the pressure gradient is greater. For this evaluation, three types of panel edge spacing were used as follows:

- Type 1, panel edges equally spaced
  - 20 panels
  - 30 panels
  - 40 panels

- Type 2, panel edges at $x/c = (1-\cos\theta)$, with θ varying from 0 to 90 degrees by equal increments
  - 10 panels
  - 12 panels
  - 14 panels
  - 20 panels

- Type 3, panel edges at x/c = ((1-cosθ)/2), with θ varying from 0 to 180 degrees by equal increments
  - 10 panels
  - 14 panels
  - 20 panels

With type 1 paneling, it is necessary to add many panels to significantly reduce the size of the panels at the leading edge. With type 2 paneling, the leading-edge panels are quite small without a lot of panels, but the panels at the trailing edge are large. With type 3 paneling, the panels at both the leading edge and the trailing edge are relatively small with a nominal number of panels.

Table 1 shows the relative error in the calculated leading-edge suction coefficient when only the first half-panel is used in the calculation. The approximate closed form formula grossly overpredicts the values as stated earlier.

Figure 1 shows the predictions for each of the types of paneling as a function of the number of points used in the summation. The 20 panel cases are shown and are typical of the trends. With both the trapezoidal rule and Simpson's rule, the value of the suction coefficient becomes smaller, and asymptotically approaches a limit, as more points are used. This change is caused by a combination of the better fit obtained by using more points and the smaller contribution from the approximate closed form formula used at the leading edge. This improves the prediction for the case with equally spaced panel edges (type 1 paneling), but not for the others. This trend—to reduce the magnitude of the leading-edge suction coefficient as more points are used—is also seen in the results using a Gaussian quadrature. The reduction is much smaller as it is not necessary to use the approximate closed form formula at the leading edge.

For paneling types 2 and 3, these results lack sufficient accuracy. Figures 2 and 3 show the downwash distribution for paneling types 1 and 2, respectively. A comparison of these figures shows that the regions where the values of downwash are nonzero are more extensive with type 2 paneling than with type 1 paneling.

As the effect of the logarithmic singularity in the downwash distribution at panel edges is accounted for in the Gaussian quadrature method, this method was used to determine the effect of including more half-panels (always an odd number) in the calculation. The relative error in the calculation of leading-edge suction is summarized in table 2 for integration over one to nine half-panels. As more half-panels are included, the number of points per half-panel becomes even less important.

These data are shown in figure 4 as a function of the fraction of chord length included in the summation and in figure 5 as a function of the number of half-panels used in the calculation. In both figures, the data shown were obtained by using nine points per half-panel. It is clear that the number of half-panels used is much more important than the fraction of the chord length included in the summation.

For all three types of paneling studied, it is clear that the integration should be over more than the first half-panel. However, as more half-panels are added, the incremental effect of each becomes smaller and smaller.

It has become apparent that the accuracy of this calculation varies with the following parameters.

1. The panel edge spacing and the number of panels in the solution

2. The type of integration and the number of points used

3. The number of panels and, therefore, the fraction of chord length, included in the integration

The calculations are consistently more influenced by the type of panel edge spacing than by the number of panels. Integration over only the first half-panel is not sufficiently accurate, although the results are similar using all three methods—trapizoidal rule, Simpson's rule, and Gaussian quadrature. A limit is approached asymptotically when more points are used with any of these methods.

Because the Gaussian quadrature was derived for a logarithmic singularity at the panel edge, it was the only method used for the summation over more than one-half panel. The number of panels included in the the summation is a more important parameter than the fraction of chord over which the summation is made. A definite improvement in the prediction is seen as more panels are used. The results asymptotically approach a limit with integration to the center of the third panel.

In conclusion, reasonable accuracy for the two-dimensional case is obtained using the Gaussian quadrature with six points per half-panel from the section leading edge to the control point (center) of the third panel.

USE IN A THREE-DIMENSIONAL ANALYSIS

The method developed in the previous sections could be used to obtain the leading-edge suction coefficient distribution on a three-dimensional wing by treating the centerline of each strip of panels as if it were a two-dimensional plate.

The necessary data are available in the LEV Program when a solution for attached-flow is requested. This method uses the current capability in the LEV Program for evaluating flow field properties at points other than the control points (off-body points). For this study, which was performed using code for a two-dimensional model, the effect of the following variations were studied:

- Panel spacing along the chord
- Type of summation
  - Trapezoidal rule
  - Simpson's rule
  - Gaussian quadrature, using an equation that specifies a logarithmic singularity at the panel edge
- Number of points, and number of half-panels included in the summation

Whereas, each type of summation gave satisfactory results for some specific paneling, the Gaussian quadrature using six points per half-panel to the control point of the third panel gave consistently good results for all the panelings used in the study.

For each row of panels, the additions required to the LEV Program are as follows:

- A routine to determine the locations (x, y, and z) of off-body points to be evaluated, and the weighting factor to be applied to the data at each point in calculating the leading-edge suction
- A routine to calculate the leading-edge suction after the solution is completed

An evaluation of this method in a three-dimensional environment was not made. Some modifications may be necessary at that time.

Boeing Commercial Airplane Company
P.O. Box 3707
Seattle, Washington 98124
May 23, 1983

REFERENCES

1. Wery, Andre C.; and Kulfan, Robert M.: Aeroelastic Loads Prediction for an Arrow Wing. Task II - Evaluation of Semi-Empirical Methods. NASA CR-3641, 1983.

2. Dusto, A. R.; et al.: A Method for Predicting the Stability Characteristics of an Elastic Airplane. Volume I - FLEXSTAB Theoretical Description. NASA CR-114712, 1974.

3. Johnson, F. T.; Lu, P.; Tinoco, E. N.; and Epton, M. A.: An Improved Panel Method for the Solution of Three-Dimensional Leading-Edge Vortex Flows, Volume I - Theory Document. NASA CR-3278, 1980.

4. Tinoco, E. N.; Lu, P.; and Johnson, F. T.: An Improved Panel Method for the Solution of Three-Dimensional Leading-Edge Vortex Flows, Volume II - User's Guide and Programmer's Document. NASA CR-3279, 1980.

5. Ehlers, F. Edward; Epton, Michael A.; Johnson, Forrester T.; Magnus, Alfred E.; and Rubbert, Paul E.: A Higher Order Panel Method for Linearized Supersonic Flow. NASA CR-3062, 1979.

6. Desmarais, R. N.: Programs for Computing Abscissas and Weights for Classical and Nonclassical Gaussian Quadrature Formulas. NASA TN D-7924, 1975.

Table 1.—A Summary of Relative Error in the Calculated Value of Leading-Edge Suction Coefficient, Integration Over One Half-Panel of Two-Dimensional Flat Plate, M = 0.0

(a) Approximate Closed Form Formula

No. of panels	Fraction of chord	Closed form					
Panel edges equally spaced							
20	0.02500	0.47303					
30	0.01667	0.55139					
40	0.01250	0.60595					
Panel edges at x/c = (1 - cos θ), θ varying from 0 to 90 degrees in equal increments							
10	0.00616	0.50054					
12	0.00428	0.56449					
14	0.00314	0.61865					
20	0.00154	0.74322					
Panel edges at x/c = ((1 - cos θ)/2), θ varying from 0 to 180 degrees in equal increments							
10	0.01224	0.43794					
14	0.00627	0.54265					
20	0.00308	0.65699					

(b) Trapezoidal Rule

No. of panels	Fraction of chord	Number of points per half-panel					
		5	7	9	11	13	15
Panel edges equally spaced							
20	0.02500	0.06705	0.05372	0.04738	0.04376	0.04145	0.03986
30	0.01667	0.07511	0.06016	0.05314	0.04918	0.04667	0.04495
40	0.01250	0.07992	0.06383	0.05634	0.05213	0.04948	0.04767
Panel edges at x/c = (1 - cos θ), θ varying from 0 to 90 degrees in equal increments							
10	0.00616	-0.11107	-0.12851	-0.13645	-0.14083	-0.14355	-0.14537
12	0.00428	-0.10531	-0.12411	-0.13262	-0.13729	-0.14017	-0.14210
14	0.00314	-0.10053	-0.12048	-0.12947	-0.13439	-0.13742	-0.13943
20	0.00154	-0.09022	-0.11284	-0.12295	-0.12843	-0.13179	-0.13401
Panel edges at x/c = ((1 - cos θ)/2), θ varying from 0 to 180 degrees in equal increments							
10	0.01224	-0.08444	-0.09992	-0.10708	-0.11107	-0.11356	-0.11525
14	0.00627	-0.08394	-0.10182	-0.10997	-0.11446	-0.11725	-0.11912
20	0.00308	-0.08073	-0.10118	-0.11040	-0.11543	-0.11853	-0.12060

Table 1.—(Concluded)

(c) Simpson's Rule

No. of panels	Fraction of chord	Number of points per half-panel					
		5	7	9	11	13	15
Panel edges equally spaced							
20	0.02500	0.05001	0.04139	0.03781	0.03598	0.03491	0.03423
30	0.01667	0.05800	0.04778	0.04353	0.04136	0.04009	0.03929
40	0.01250	0.06278	0.05143	0.04671	0.04429	0.04289	0.04200
Panel edges at x/c = (1 - cos θ), θ varying from 0 to 90 degrees in equal increments							
10	0.00616	-0.12583	-0.13916	-0.14470	-0.14753	-0.14917	-0.15021
12	0.00428	-0.12012	-0.13479	-0.14089	-0.14401	-0.14581	-0.14695
14	0.00314	-0.11538	-0.13120	-0.13777	-0.14113	-0.14307	-0.14430
20	0.00154	-0.10514	-0.12361	-0.13129	-0.13520	-0.13747	-0.13891
Panel edges at x/c = ((1 - cos θ)/2), θ varying from 0 to 180 degrees in equal increments							
10	0.01224	-0.09970	-0.11094	-0.11561	-0.11800	-0.11938	-0.12026
14	0.00627	-0.09914	-0.11279	-0.11847	-0.12136	-0.12304	-0.12411
20	0.00308	-0.09589	-0.11213	-0.11887	-0.12232	-0.12431	-0.12557

(d) Gaussian Quadrature

No. of panels	Fraction of chord	Number of points per half-panel						
		3	4	5	6	7	8	9
Panel edges equally spaced								
20	0.02500	0.03527	0.03389	0.03322	0.03285	0.03262	0.03247	0.03237
30	0.01667	0.03995	0.03857	0.03791	0.03754	0.03731	0.03716	0.03705
40	0.01250	0.04239	0.04101	0.04035	0.03998	0.03975	0.03960	0.03950
Panel edges at x/c = (1 - cos θ), θ varying from 0 to 90 degrees in equal increments								
10	0.00616	-0.15084	-0.15196	-0.15250	-0.15281	-0.15299	-0.15312	-0.15320
12	0.00428	-0.14790	-0.14902	-0.14957	-0.14987	-0.15006	-0.15018	-0.15027
14	0.00314	-0.14551	-0.14664	-0.14718	-0.14749	-0.14768	-0.14780	-0.14789
20	0.00154	-0.14074	-0.14187	-0.14242	-0.14273	-0.14292	-0.14305	-0.14315
Panel edges at x/c = ((1 - cos θ)/2), θ varying from 0 to 180 degrees in equal increments								
10	0.01224	-0.12030	-0.12147	-0.12203	-0.12235	-0.12254	-0.12267	-0.12275
14	0.00627	-0.12474	-0.12590	-0.12646	-0.12677	-0.12696	-0.12709	-0.12717
20	0.00308	-0.12683	-0.12798	-0.12853	-0.12884	-0.12904	-0.12916	-0.12925

Table 2.—A Summary of Relative Error in the Calculated Value of Leading-Edge Suction Coefficient, Integration Using a Gaussian Quadrature Over Several Half-Panels of Two-Dimensional Flat Plate, M = 0.0

(a) Panel Edges Equally Spaced

No. of half-panels	Fraction of chord	Number of points per half-panel						
		3	4	5	6	7	8	9
20 Panels								
1	0.02500	0.03527	0.03389	0.03322	0.03285	0.03262	0.03247	0.03237
3	0.07500	-0.00004	-0.00102	-0.00148	-0.00174	-0.00190	-0.00200	-0.00207
5	0.12500	-0.00707	-0.00804	-0.00849	-0.00875	-0.00890	-0.00900	-0.00907
7	0.17500	-0.00817	-0.00914	-0.00959	-0.00985	-0.01000	-0.01010	-0.01017
9	0.22500	-0.00840	-0.00936	-0.00982	-0.01007	-0.01022	-0.01033	-0.01040
30 Panels								
1	0.01667	0.03995	0.03857	0.03791	0.03754	0.03731	0.03716	0.03705
3	0.05000	0.00437	0.00339	0.00293	0.00268	0.00252	0.00242	0.00235
5	0.08333	-0.00279	-0.00374	-0.00420	-0.00445	-0.00460	-0.00470	-0.00477
7	0.11667	-0.00391	-0.00487	-0.00532	-0.00557	-0.00573	-0.00583	-0.00590
9	0.15000	-0.00414	-0.00510	-0.00555	-0.00580	-0.00596	-0.00606	-0.00613
40 Panels								
1	0.01250	0.04239	0.04101	0.04035	0.03998	0.03975	0.03960	0.03950
3	0.03750	0.00667	0.00570	0.00524	0.00499	0.00483	0.00473	0.00466
5	0.06250	-0.00054	-0.00150	-0.00195	-0.00220	-0.00235	-0.00245	-0.00252
7	0.08750	-0.00168	-0.00264	-0.00309	-0.00334	-0.00349	-0.00359	-0.00366
9	0.11250	-0.00192	-0.00287	-0.00332	-0.00357	-0.00372	-0.00382	-0.00389

Table 2.–(Continued)

(b) Panel Edges at x/c = (1 - cos θ), θ Varying From 0 to 90 Degrees in Equal Increments

No. of half-panels	Fraction of chord	Number of points per half-panel						
		3	4	5	6	7	8	9
10 Panels								
1	0.00616	-0.15084	-0.15196	-0.15250	-0.15281	-0.15299	-0.15312	-0.15320
3	0.03063	-0.04680	-0.04710	-0.04719	-0.04723	-0.04725	-0.04726	-0.04726
5	0.07897	-0.02537	-0.02554	-0.02556	-0.02556	-0.02555	-0.02555	-0.02554
7	0.14999	-0.02007	-0.02021	-0.02022	-0.02021	-0.02020	-0.02019	-0.02018
9	0.24194	-0.01846	-0.01858	-0.01859	-0.01857	-0.01856	-0.01855	-0.01854
12 Panels								
1	0.00428	-0.14790	-0.14902	-0.14957	-0.14987	-0.15006	-0.15018	-0.15027
3	0.02131	-0.04286	-0.04316	-0.04325	-0.04328	-0.04330	-0.04331	-0.04332
5	0.05510	-0.02081	-0.02097	-0.02099	-0.02098	-0.02098	-0.02097	-0.02096
7	0.10505	-0.01508	-0.01521	-0.01521	-0.01520	-0.01519	-0.01518	-0.01517
9	0.17031	-0.01318	-0.01330	-0.01329	-0.01328	-0.01326	-0.01325	-0.01325
14 Panels								
1	0.00314	-0.14551	-0.14664	-0.14718	-0.14749	-0.14768	-0.14780	-0.14789
3	0.01568	-0.03979	-0.04008	-0.04016	-0.04020	-0.04022	-0.04023	-0.04024
5	0.04059	-0.01733	-0.01749	-0.01750	-0.01750	-0.01749	-0.01749	-0.01748
7	0.07757	-0.01134	-0.01147	-0.01147	-0.01145	-0.01144	-0.01143	-0.01142
9	0.12615	-0.00927	-0.00938	-0.00938	-0.00936	-0.00934	-0.00933	-0.00933
20 Panels								
1	0.00154	-0.14074	-0.14187	-0.14242	-0.14273	-0.14292	-0.14305	-0.14315
3	0.00770	-0.03379	-0.03408	-0.03416	-0.03420	-0.03422	-0.03424	-0.03425
5	0.01997	-0.01073	-0.01087	-0.01088	-0.01088	-0.01088	-0.01088	-0.01088
7	0.03829	-0.00435	-0.00446	-0.00446	-0.00444	-0.00443	-0.00443	-0.00443
9	0.06253	-0.00202	-0.00212	-0.00211	-0.00209	-0.00208	-0.00207	-0.00207

Table 2.—(Concluded)

(c) Panel Edges at x/c = ((1 - cos θ)/2), θ Varying From 0 to 180 Degrees in Equal Increments

No. of half-panels	Fraction of chord	Number of points per half-panel						
		3	4	5	6	7	8	9
10 Panels								
1	0.01224	-0.12030	-0.12147	-0.12203	-0.12235	-0.12254	-0.12267	-0.12275
3	0.05998	-0.01797	-0.01831	-0.01842	-0.01847	-0.01850	-0.01852	-0.01853
5	0.15080	-0.00060	-0.00082	-0.00087	-0.00088	-0.00089	-0.00089	-0.00089
7	0.27580	0.00148	0.00128	0.00125	0.00124	0.00124	0.00124	0.00124
9	0.42275	0.00116	0.00097	0.00094	0.00093	0.00093	0.00094	0.00094
14 Panels								
1	0.00627	-0.12474	-0.12590	-0.12646	-0.12677	-0.12696	-0.12709	-0.12717
3	0.03103	-0.01925	-0.01957	-0.01966	-0.01971	-0.01973	-0.01974	-0.01975
5	0.07930	0.00130	0.00112	0.00109	0.00109	0.00109	0.00109	0.00110
7	0.14867	0.00565	0.00550	0.00548	0.00549	0.00549	0.00550	0.00551
9	0.23566	0.00661	0.00647	0.00646	0.00646	0.00647	0.00648	0.00649
20 Panels								
1	0.00308	-0.12683	-0.12798	-0.12853	-0.12884	-0.12904	-0.12916	-0.12925
3	0.01531	-0.01960	-0.01990	-0.01999	-0.02003	-0.02005	-0.02006	-0.02007
5	0.03948	0.00263	0.00247	0.00245	0.00245	0.00246	0.00247	0.00247
7	0.07499	0.00822	0.00809	0.00809	0.00810	0.00811	0.00812	0.00813
9	0.12097	0.00999	0.00987	0.00988	0.00989	0.00990	0.00991	0.00992

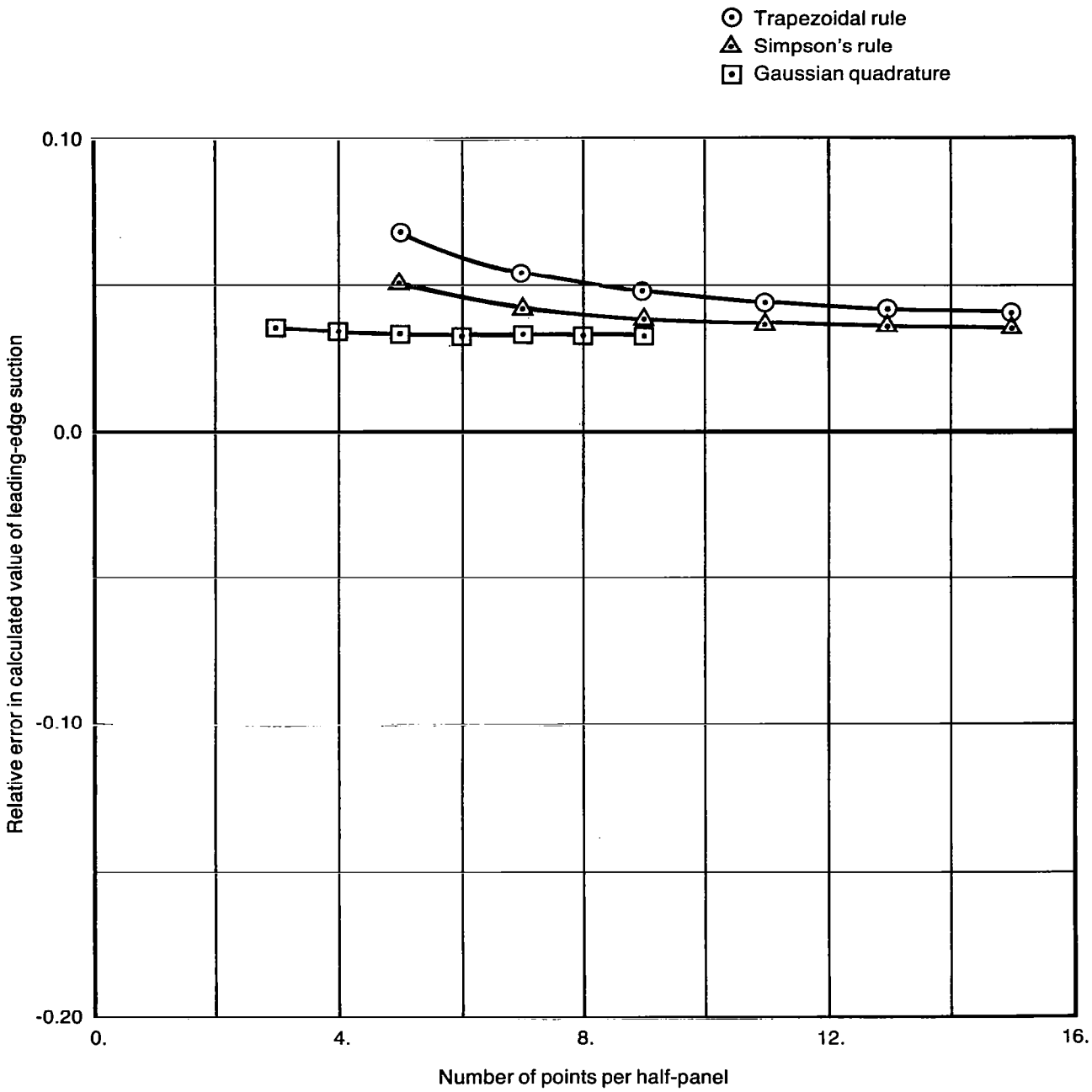

(a) Panel Edges Equally Spaced

Figure 1.–Relative Error of Calculated Values of Leading-Edge Suction as a Function of Number of Points Used in Summation, Integration Over One Half-Panel, Chord Length Divided Into 20 Panels, M = 0.0

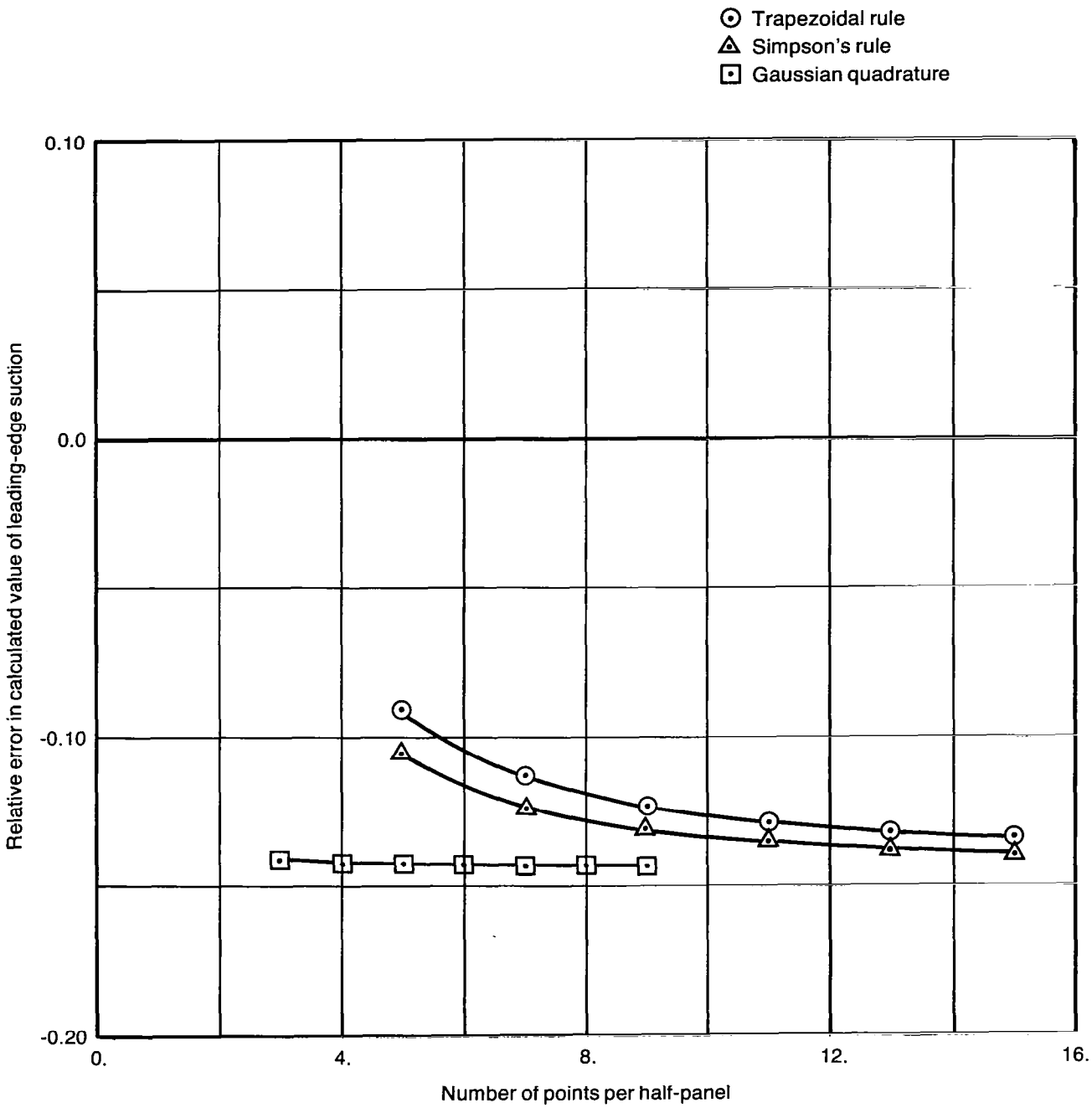

(b) Panel Edges at x/c = (1 - cos θ), θ Varying From 0 to 90 Degrees in Equal Increments

Figure 1.—(Continued)

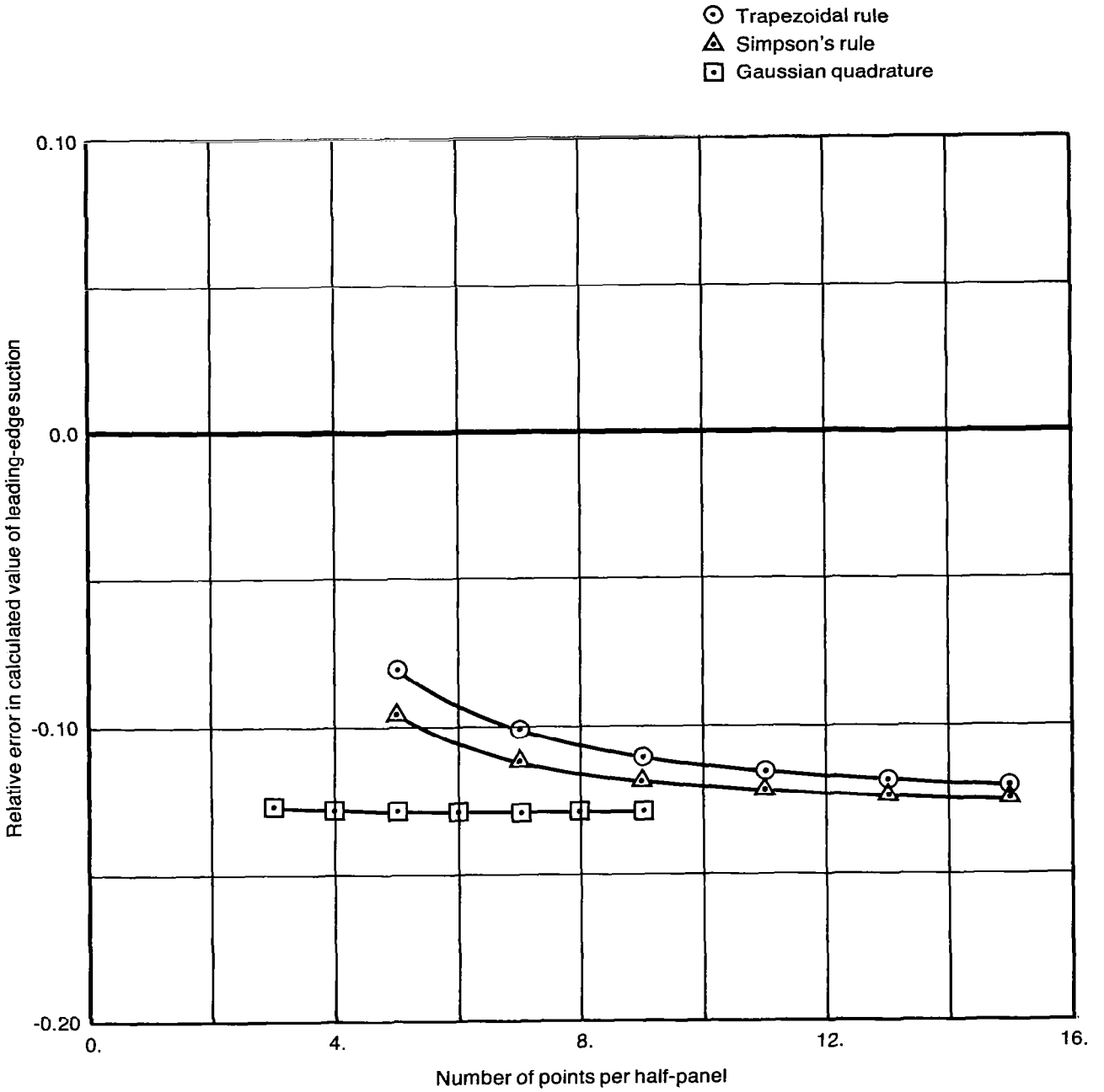

(c) Panel Edges at x/c = ((1 - cos θ) /2.), θ Varying From 0 to 180 Degrees in Equal Increments

Figure 1. – (Concluded)

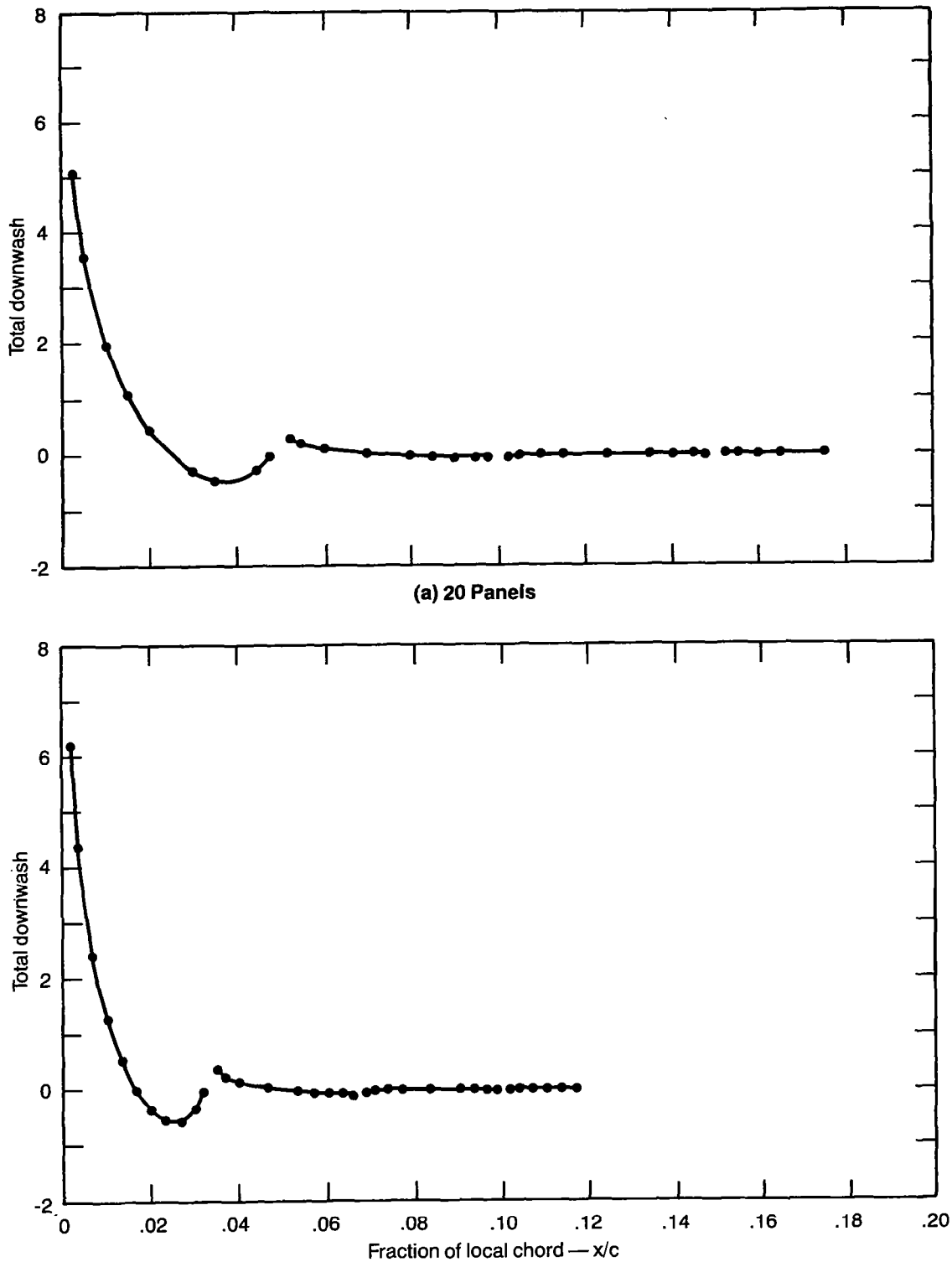

Figure 2.–Chordwise Distribution of Total Downwash for Uniform Panel Spacing, $M = 0.0$, $\alpha = 25$ Degrees

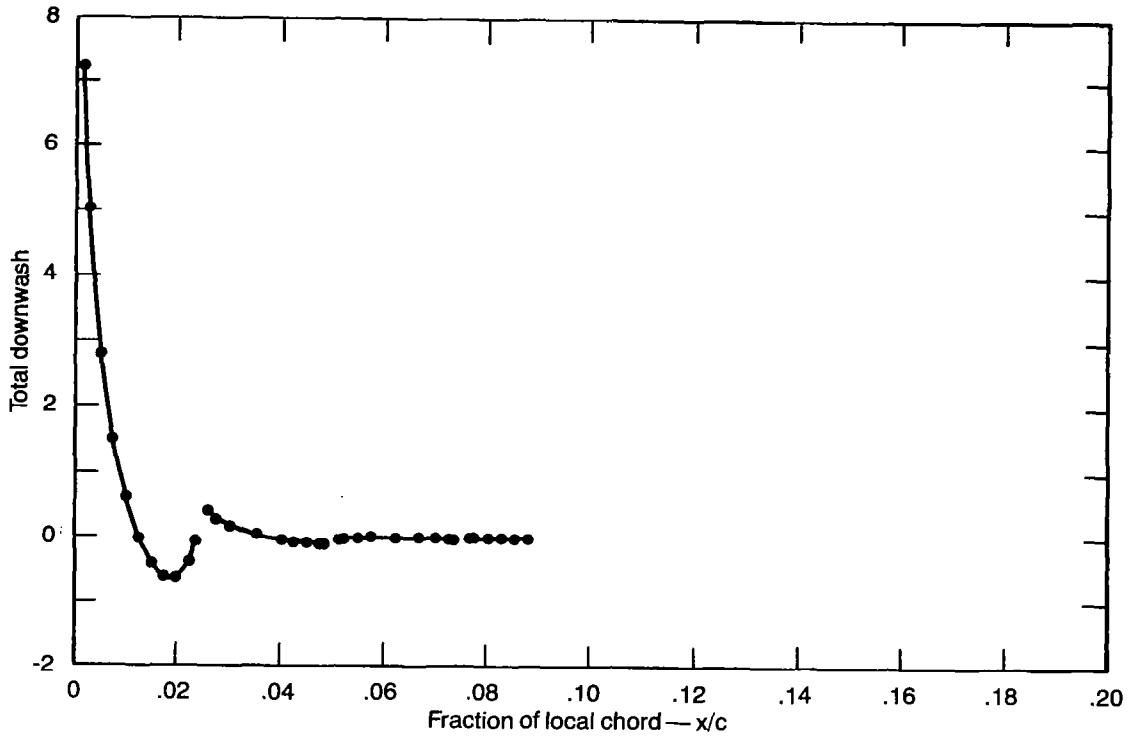

(c) 40 Panels

Figure 2.–(Concluded)

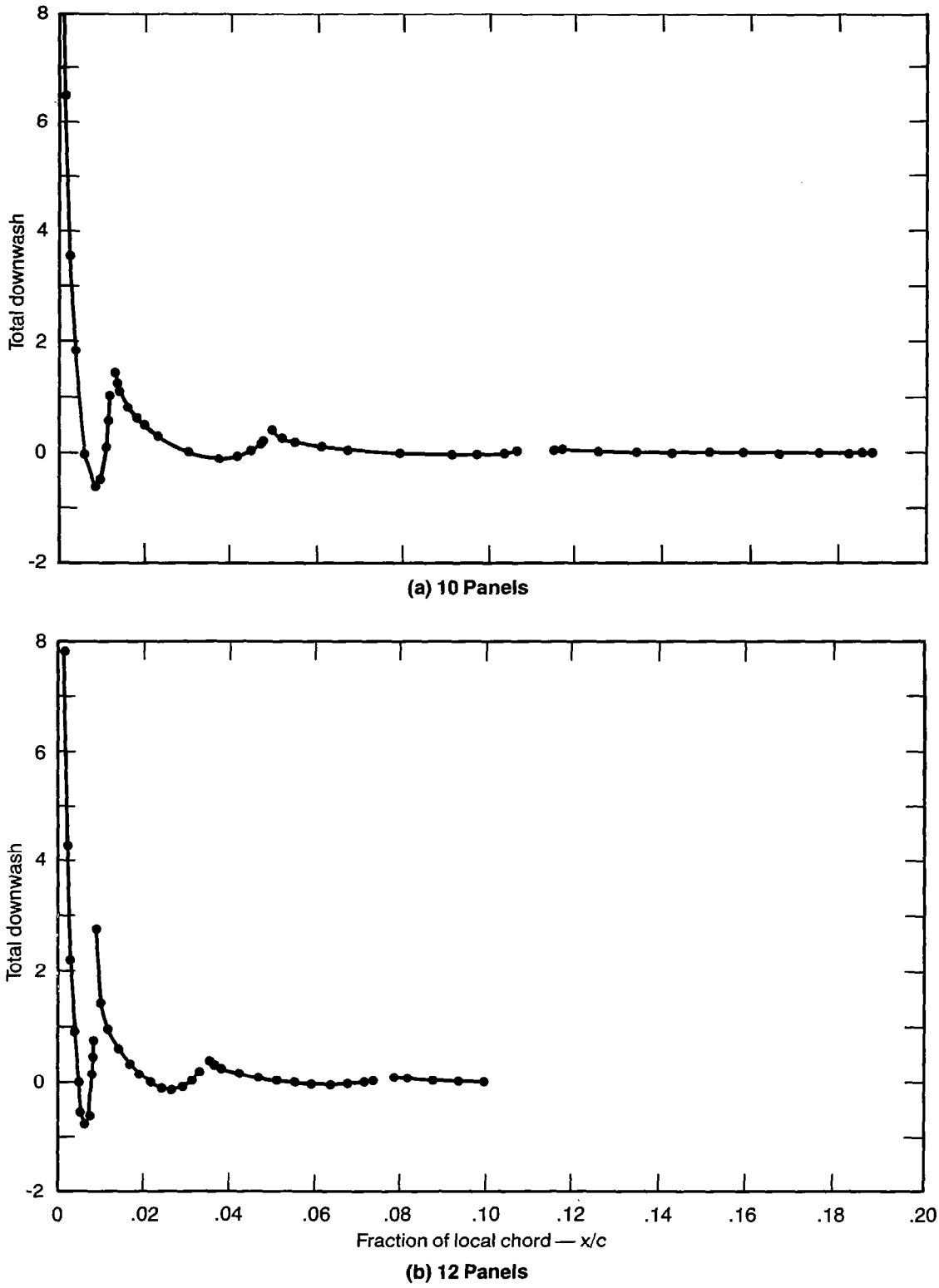

Figure 3.–Chordwise Distribution of Total Downwash for Cosine Panel Spacing, $M = 0.0$, $\alpha = 25$ Degrees

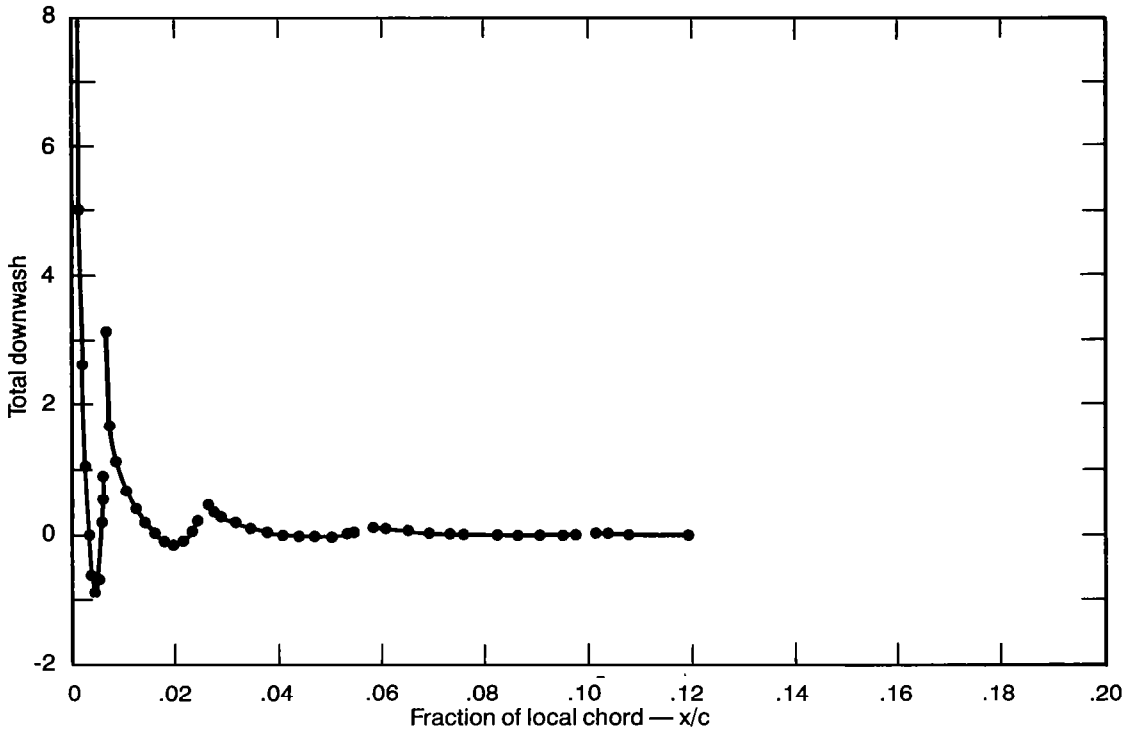

(c) 14 Panels

Figure 3.–(Concluded)

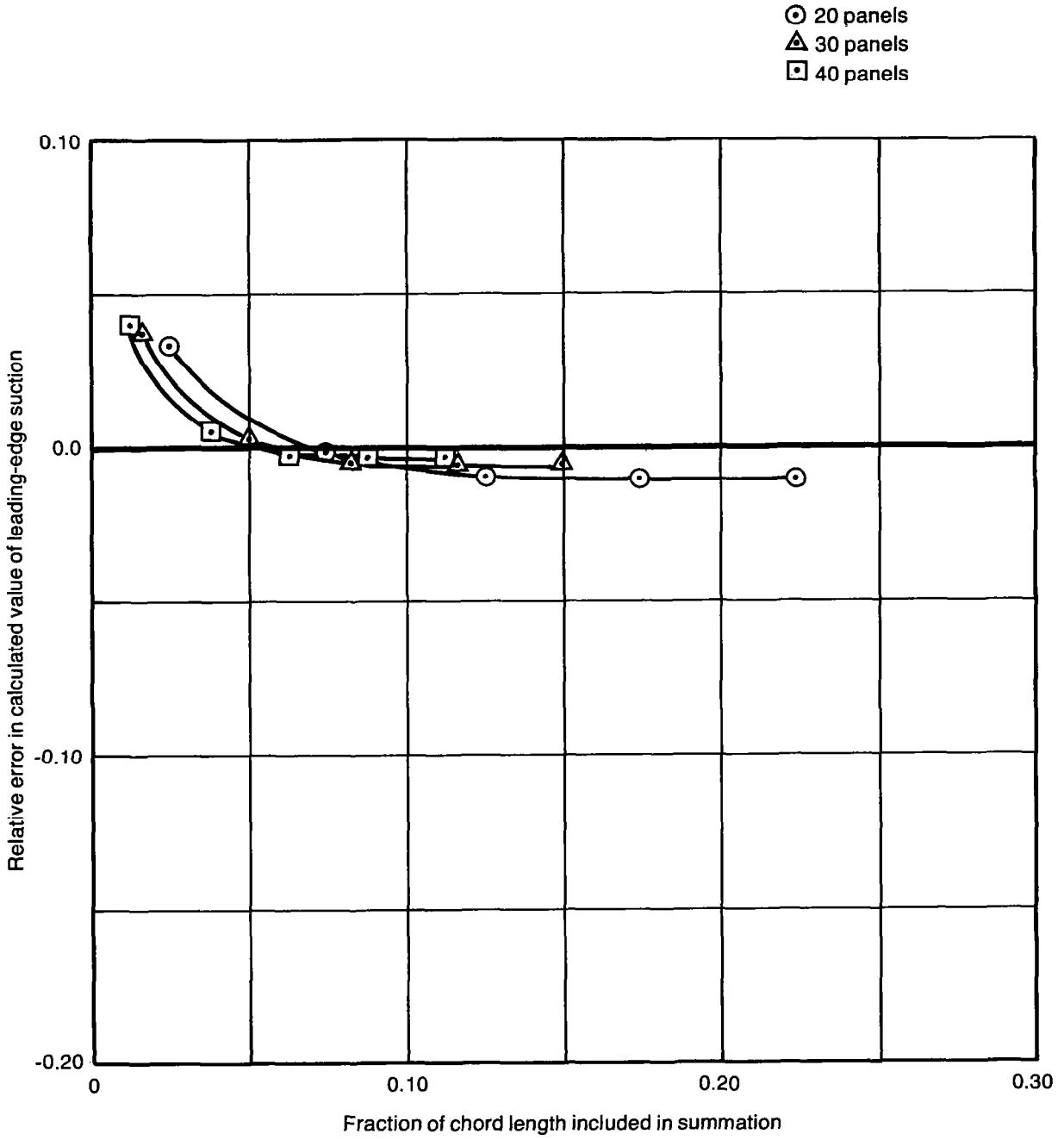

(a) Panel Edges Equally Spaced

Figure 4. – Relative Error of Calculated Values of Leading-Edge Suction as a Function of Fraction of Chord Length Used in Summation, Gaussian Quadrature, Nine Points per Half-Panel, M = 0.0

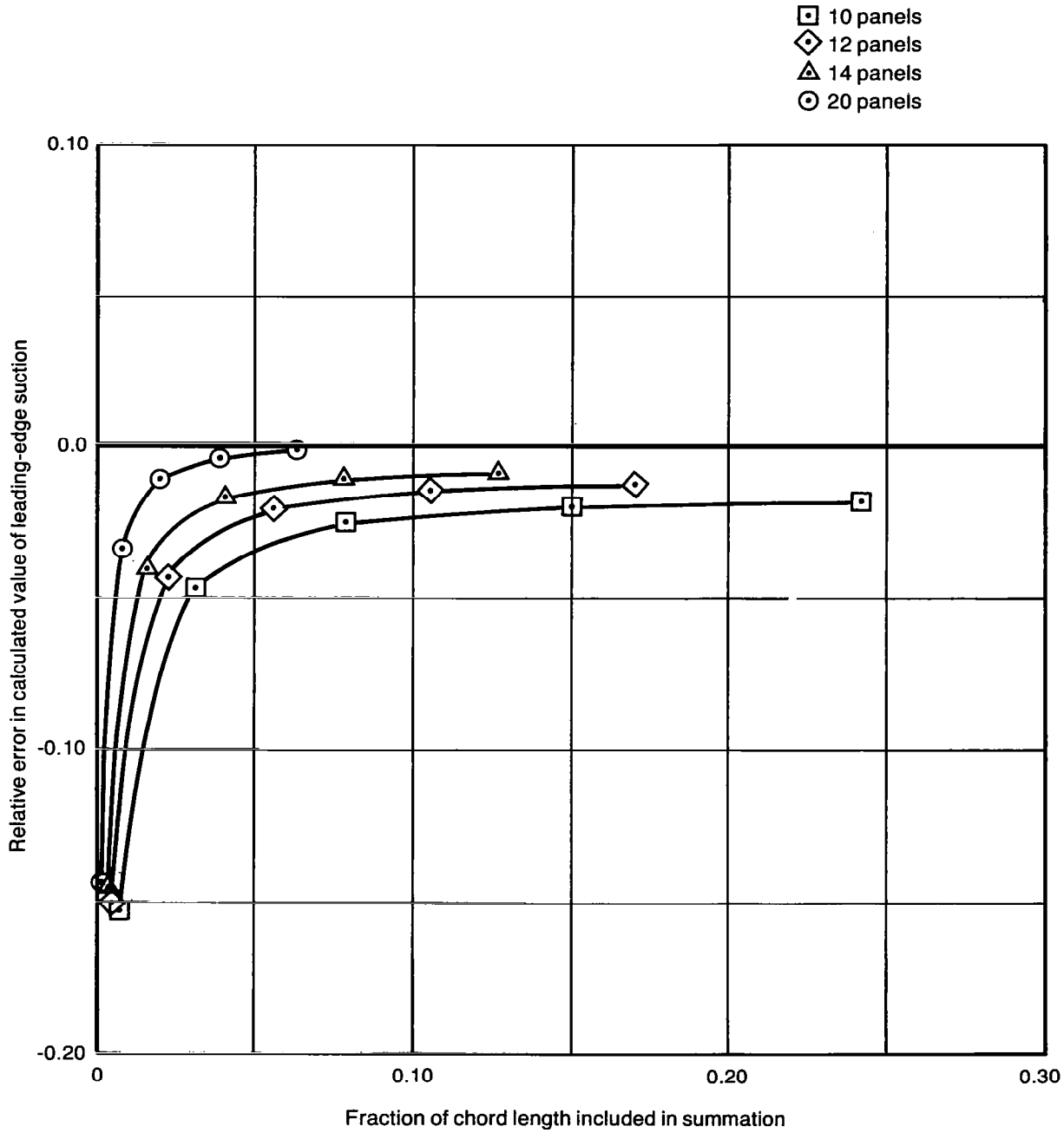

(b) Panel Edges at x/c = (1 - cos θ), θ Varying From 0 to 90 Degrees in Equal Increments

Figure 4.—(Continued)

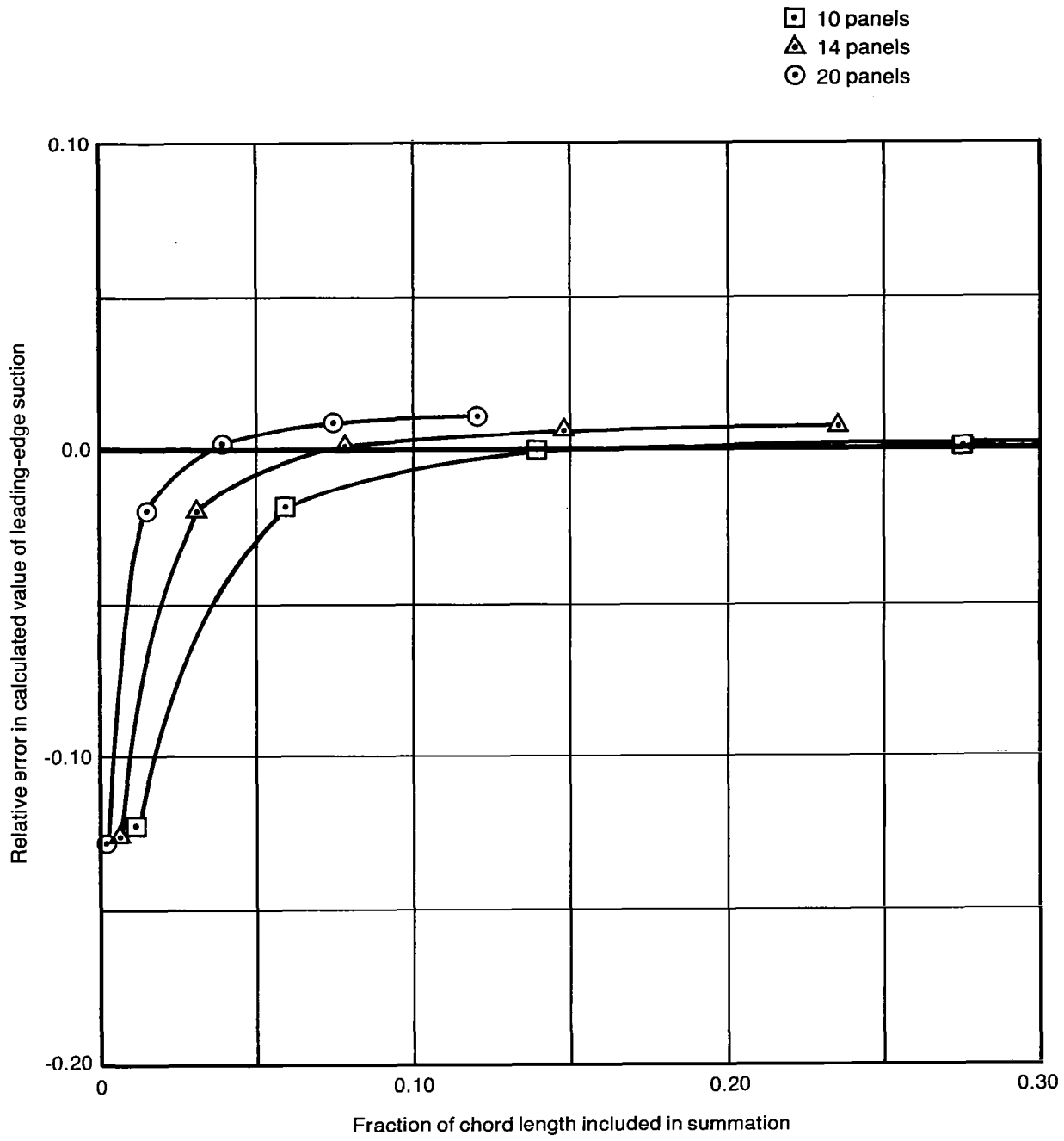

(c) Panel Edges at x/c = ((1 - cos θ) /2.), θ Varying From 0 to 180 Degrees in Equal Increments

Figure 4.–(Concluded)

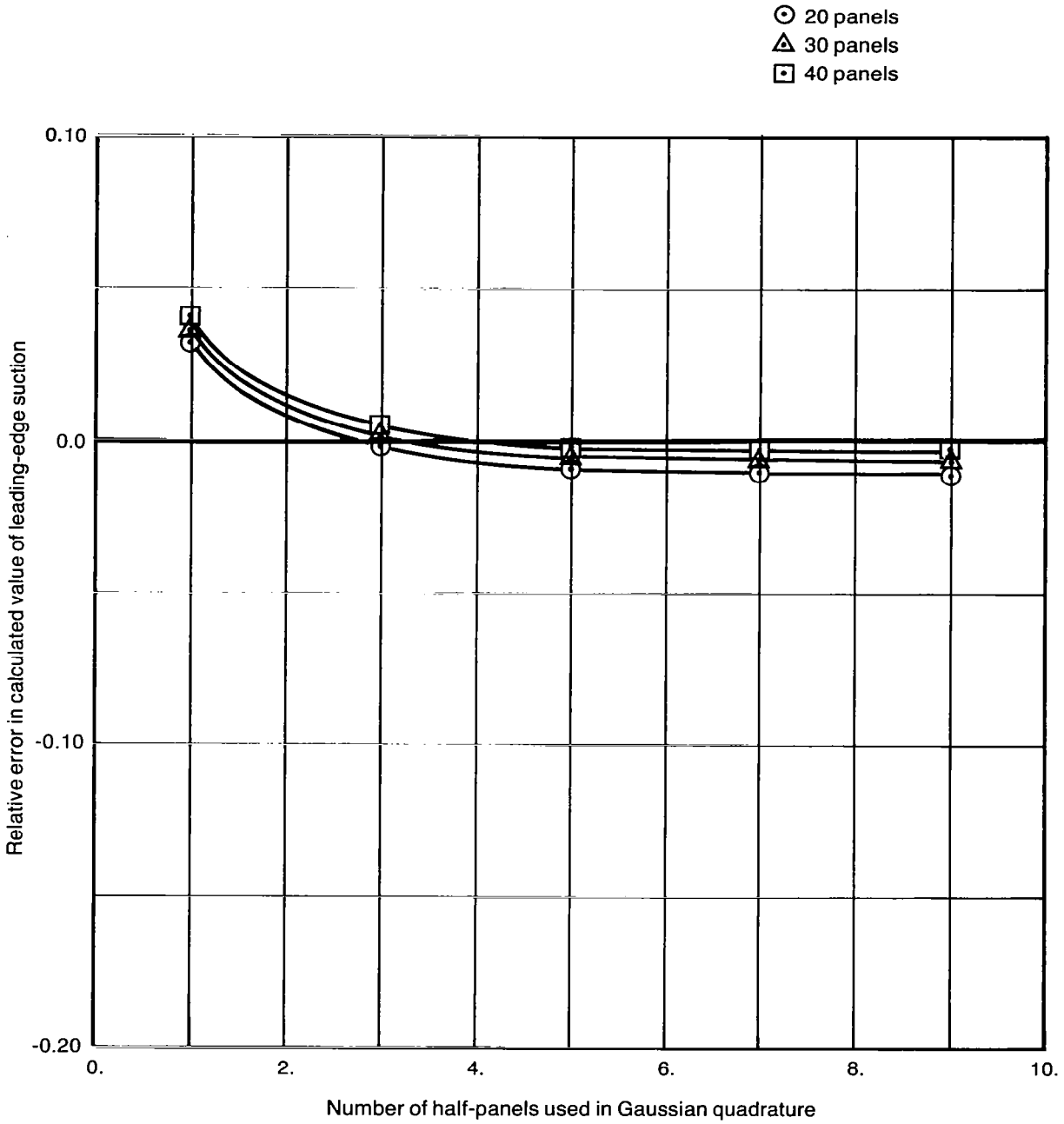

(a) Panel Edges Equally Spaced

Figure 5.—Relative Error of Calculated Values of Leading-Edge Suction as a Function of Number of Half-Panels Used in Summation, Gaussian Quadrature, Nine Points per Half-Panel, M = 0.0

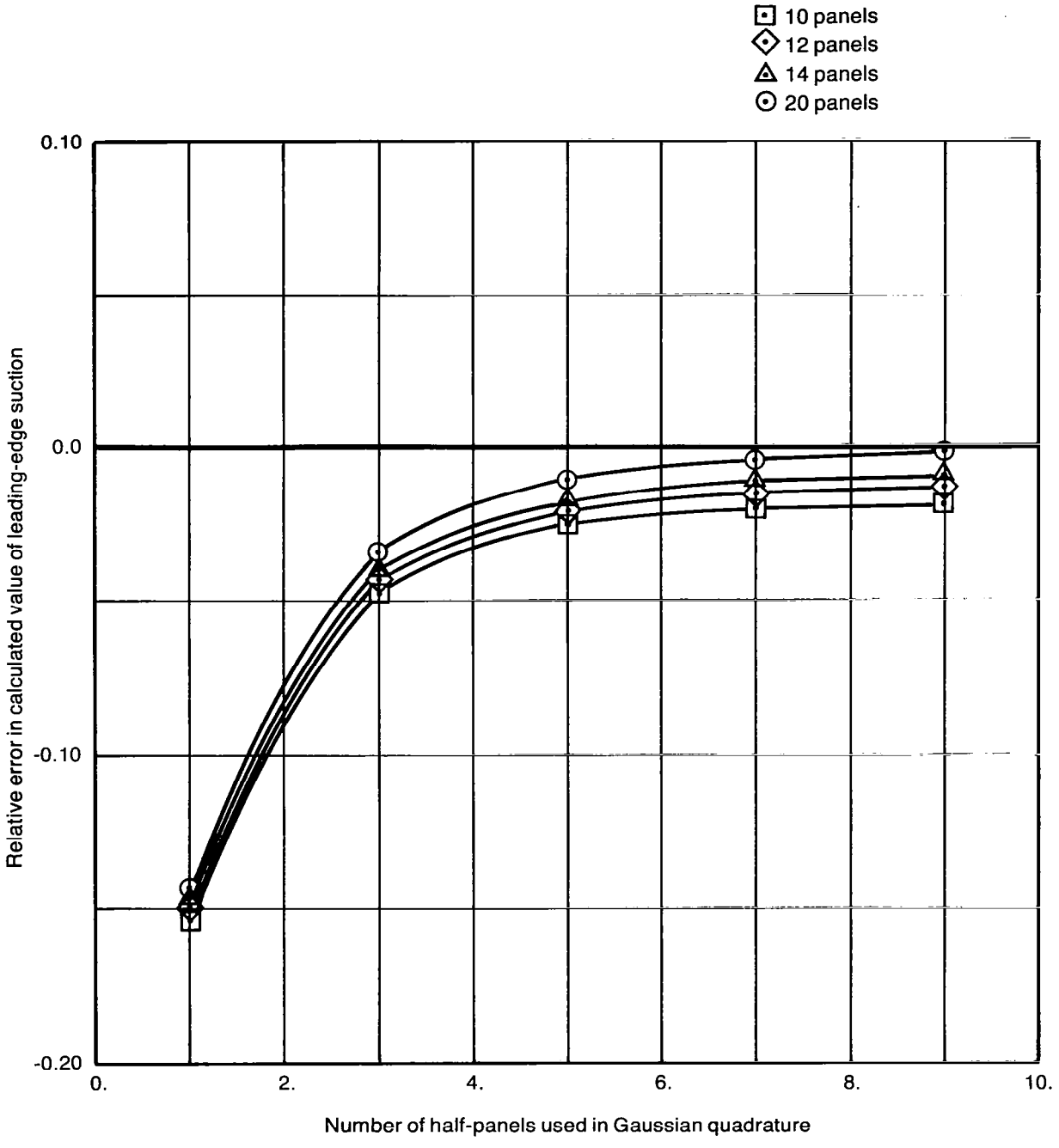

(b) Panel Edges at x/c = (1 - cos θ), θ Varying From 0 to 90 Degrees in Equal Increments

Figure 5.–(Continued)

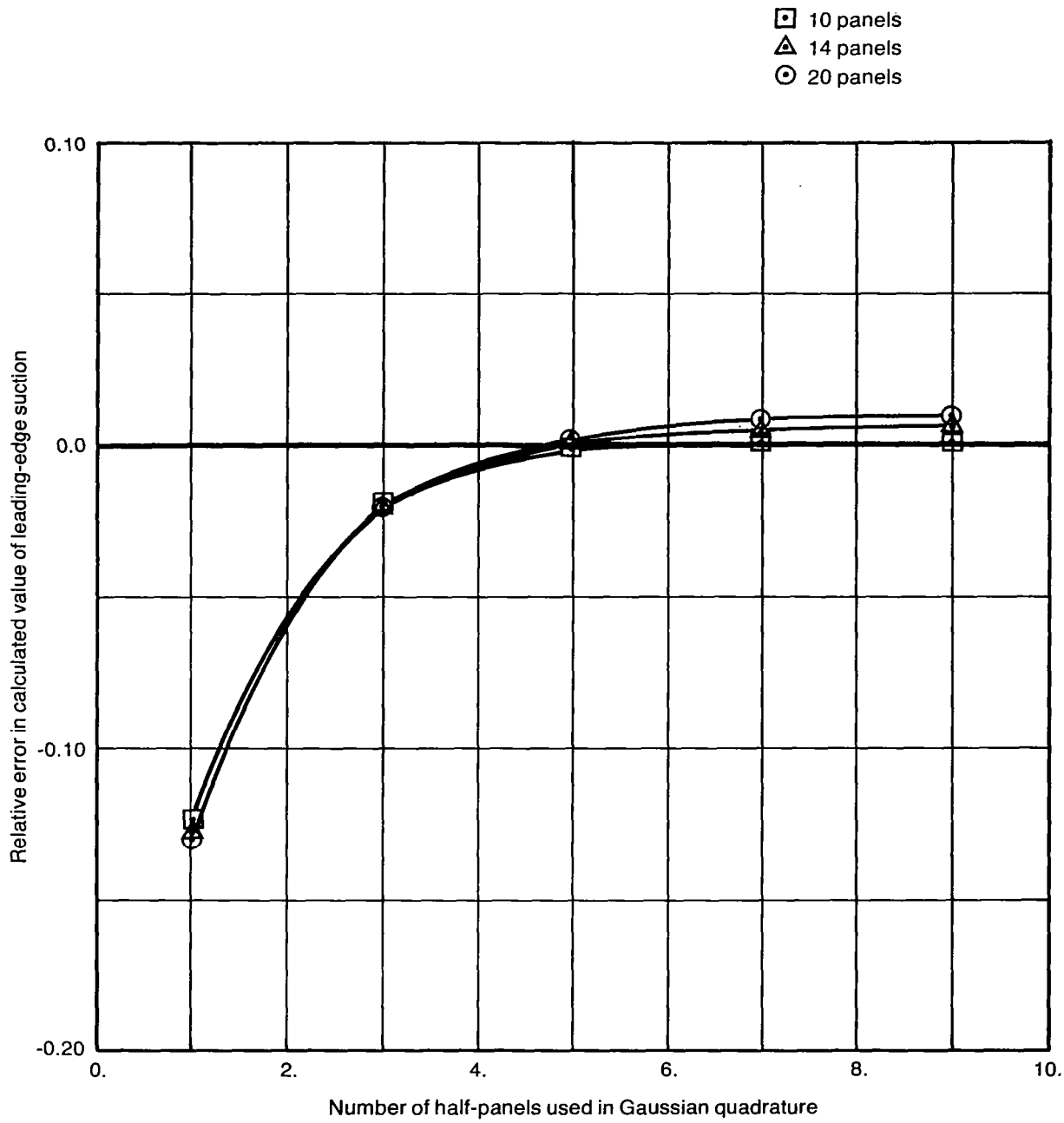

(c) Panel Edges at x/c = ((1 - cos θ) /2.), θ Varying From 0 to 180 Degrees in Equal Increments

Figure 5.—(Concluded)

1. Report No.	2. Government Accession No.	3. Recipient's Catalog No.
NASA CR-3730		

4. Title and Subtitle	5. Report Date
A METHOD FOR COMPUTING THE LEADING-EDGE SUCTION IN A HIGHER-ORDER PANEL METHOD	March 1984
	6. Performing Organization Code
7. Author(s)	8. Performing Organization Report No.
F. Edward Ehlers and Marjorie E. Manro	D6-52135
	10. Work Unit No.
9. Performing Organization Name and Address	
Boeing Commercial Airplane Company P.O. Box 3707 Seattle, Washington 98124	11. Contract or Grant No. NAS1-16740
	13. Type of Report and Period Covered Contractor Report
12. Sponsoring Agency Name and Address	
National Aeronautics and Space Administration Washington, D.C. 20546	14. Sponsoring Agency Code 743-01-12-02

15. Supplementary Notes

Technical monitor—Percy J. Bobbitt, Chief, Transonic Aerodynamics Division, NASA Langley Research Center, Hampton, Virginia.
Principal investigator—Marjorie E. Manro, Boeing Commercial Airplane Company.

16. Abstract

Experimental data show that the phenomenon of a separation-induced leading-edge vortex is influenced by the wing thickness and the shape of the leading edge. Both thickness and leading-edge shape (rounded rather than pointed) delay the formation of a vortex. Existing computer programs used to predict the effect of a leading-edge vortex do not include a procedure for determining whether or not a vortex actually exists. Studies under NASA Contract NAS1-15678 have shown that the vortex development can be predicted by using the relationship between the leading-edge suction coefficient and the parabolic nose drag. The linear theory FLEXSTAB was used to calculate the leading-edge suction coefficient.

This report describes the development of a method for calculating leading-edge suction using the capabilities of the higher-order panel methods (exact boundary conditions). For a two-dimensional case, numerical methods were developed using the doublet strength and downwash distribution along the chord.

A Gaussian quadrature formula that directly incorporates the logarithmic singularity in the downwash distribution, at all panel edges, was found to be the best method.

17. Key Words (Suggested by Author(s))	18. Distribution Statement
Aeroelasticity Aerodynamic theory Arrow-wing configuration Leading-edge suction	Unclassified-unlimited Subject category 02

19. Security Classif. (of this report)	20. Security Classif. (of this page)	21. No. of Pages	22. Price
Unclassified	Unclassified	42	A03

For sale by the National Technical Information Service, Springfield, Virginia 22151

NASA-Langley, 1984